Eur. Phys. J. B **38**, 59–64 (2004)
DOI: 10.1140/epjb/e2004-00099-7

THE EUROPEAN PHYSICAL JOURNAL B

Interface transparency of Nb/Pd layered systems

C. Cirillo, S.L. Prischepa[a], M. Salvato, and C. Attanasio[b]

Dipartimento di Fisica "E.R. Caianiello" and INFM, Università degli Studi di Salerno, Baronissi (Sa), 84081, Italy

Received 17 July 2003 / Received in final form 12 December 2003
Published online 20 April 2004 –

Abstract. We have investigated, in the framework of proximity effect theory, the interface transparency $\mathcal{T}$ of superconducting/normal metal layered systems which consist of Nb and high paramagnetic Pd deposited by dc magnetron sputtering. The obtained $\mathcal{T}$ value is relatively high, as expected by theoretical arguments. This leads to a large value of the ratio d_s^{cr}/ξ_s although Pd does not exhibit any magnetic ordering.

PACS. 74.45.+c Proximity effects; Andreev effect; SN and SNS junctions – 74.78.Fk Multilayers, superlattices, heterostructures

1 Introduction

Interface transparency $\mathcal{T}$ of artificial layered systems is an interesting issue of study, both for its fundamental and practical consequences and many papers have been recently devoted to this topic [1–4]. From one side, in fact, $\mathcal{T}$ is related to differences between Fermi velocities and band-structures of the two metals. On the other hand it is an essential parameter to take into account in the study of depairing currents [5] and quasiparticle injection devices [6–9] where high interface transparency is an important ingredient.

In this article we performed a proximity effect study of Nb/Pd layered system [10] taking into account the essential ingredient of interface transparency. We chose Nb as superconducting material and Pd as normal metal. The choice of Nb was related to its highest critical temperature among the superconducting elements while, among normal metals, Pd is the one with the larger spin susceptibility [11] which leads to giant magnetic moments in some dilute Pd alloys [12]. Moreover, by theoretical argument based on Fermi velocities and band-structures mismatch, we expected a more transparent interface than in other superconductor/normal metal combinations, such as, for example, Nb/Cu [13].

2 Theoretical background

When a superconductor (S) comes into contact with another material (X) proximity effect occurs. The other material can be a superconductor with a lower transition temperature (S'), a normal metal (N), a ferromagnet (F) or a spin glass (M). In any case there is a mutual influence which depresses superconductivity in S and induces superconductivity in X. Since at the interface the order parameter decreases in S over the coherence length ξ_s, it is necessary a minimum thickness of the S layer, d_s, to make superconductivity appear. If d_s is small the order parameter cannot reach its maximum value and the critical temperature T_c of the system is reduced, until d_s becomes too thin and superconductivity is lost. The thickness at which it happens is called critical thickness, d_s^{cr}. On the other hand, Cooper pairs coming from S penetrate X, but they are broken up over a characteristic length ξ_x, depending on the pair breaking mechanism in X. At finite temperature pairs loose their phase coherence by thermal fluctuations: this is the only pair breaking mechanism present in N metals, and lead to a temperature dependent characteristic distance, $\xi_n(T)$, which can become large at low temperatures. In magnetic metals pair breaking is due to the exchange energy E_{ex} which acts on the spin of the Cooper pairs. For strong magnets, such as Fe, $E_{ex} \gg k_B T$: this leads to a few Angstrom temperature independent coherence length ξ_F in the magnetic layer [1,14,15].

Anyway interfaces between different metals are never fully transparent with the result that proximity effect is somehow screened, because electrons coming from S are reflected rather than transmitted in X. A finite transparency gives rise, for example, to a smaller d_s^{cr}. This may be due to interface imperfections, lattice mismatches, fabrication method [4,16], but also to intrinsic effects such as difference between Fermi velocities and band-structures of the two metals [13]. The interface transparency due to Fermi velocities mismatches in the free electron model, is

[a] *Permanent address*: State University of Computer Science and RadioElectronics, P. Brovka street 6, 220600, Minsk, Belarus
[b] e-mail: attanasio@sa.infn.it

given by [1,19]:

$$\mathcal{T} = \frac{4k_x k_s}{[k_x + k_s]^2} \quad (1)$$

where $k_{x,s} = mv_{x,s}/\hbar$ are the projections of Fermi wave vectors of X and S metals on the direction perpendicular to the interface. Moreover for the magnetic case the situation is more complicated due to the role played by the splitting of the spin subbands and the spin-dependent impurity scattering [17].

The starting point for a complete description of proximity effect in multilayers, valid for arbitrary transparency, was given by Kupriyanov and Lukichev [18] in the framework of Usadel equations (dirty limit). In particular, the model we used to describe the dependence $T_c(d_s)$ for N/S/N trilayers is based on the Werthamer approximation, valid for not too low temperatures, provided the boundary transparency is sufficiently small [19]. In this limit the system of algebraic equations to determine T_c is:

$$\Omega_1 \tan\left(\frac{\Omega_1 d_S}{2\xi_S}\right) = \frac{\gamma}{\gamma_b} \quad (2)$$

$$\Psi\left(\frac{1}{2} + \frac{\Omega_1^2 T_{cs}}{2T_c}\right) - \Psi\left(\frac{1}{2}\right) = \ln\left(\frac{T_{cs}}{T_c}\right), \frac{T_c}{T_{cs}} \gg \frac{\gamma}{\gamma_b} \quad (3)$$

with the identification of the Abrikosov-Gorkov pair-breaking parameter $\rho{=}\pi T_c \Omega_1^2 = \pi T_c(\gamma/\gamma_b)(2\xi_s/d_s)$ where $\Psi(x)$ is the digamma function and T_{cs} is the bulk critical temperature of the S layer. These equations contain two parameters γ and γ_b defined as

$$\gamma = \frac{\rho_s \xi_s}{\rho_n \xi_n}, \gamma_b = \frac{R_B}{\rho_n \xi_n} \quad (4)$$

where ρ_s and ρ_n are the low temperature resistivities of S and N, respectively, while R_B is the normal-state boundary resistivity times its area. The parameter γ is a measure of the strength of the proximity effect between the S and N metals and can be determined experimentally by measuring $\rho_s \equiv \rho_{\mathrm{Nb}}$, $\rho_n \equiv \rho_{\mathrm{Pd}}$, $\xi_s \equiv \xi_{\mathrm{Nb}}$ and $\xi_n \equiv \xi_{\mathrm{Pd}}$. The parameter γ_b, instead, describes the effect of the boundary transparency $\mathcal{T}$, to which it is roughly related by

$$\mathcal{T} = \frac{1}{1 + \gamma_b}. \quad (5)$$

Due to its dependence on R_B, which is difficult to measure, γ_b (or $\mathcal{T}$) can't be determined experimentally, so it was extracted by a fitting procedure.

3 Experimental results

The samples were grown on Si(100) substrates by a dual-source magnetically enhanced dc triode sputtering system and they consist of Nb layers ($T_c \approx 8.8$ K) and Pd layers. The deposition conditions were similar to those of the Nb/Pd multilayers earlier described [10] except for the fact that the 8 samples, obtained in a single deposition run, were not heated. Three different sets of multilayers were prepared. Two sets (set A and set B), built as follows, $d_{\mathrm{Pd}}/d_{\mathrm{Nb}}/d_{\mathrm{Pd}}$, were used to determine $d_s^{cr} \equiv d_{\mathrm{Nb}}^{cr}$ by the variation of T_c as function of the Nb layer thickness. Here d_{Pd} was fixed at around 1500 Å in order to represent a half-infinite layer, while d_{Nb} was variable from 200 to 1300 Å. The third set (set C) was used to estimate ξ_{Pd} by the variation of T_c with d_{Pd}. Now the samples were made up of five layers: $d_{\mathrm{Pd}}^{out}/d_{\mathrm{Nb}}/d_{\mathrm{Pd}}^{in}/d_{\mathrm{Nb}}/d_{\mathrm{Pd}}^{out}$, with the outer Pd layers of 300 Å in order to create a symmetric situation for the Nb layers, with d_{Nb} fixed at 500 Å, while d_{Pd}^{in} was varied from 50 to 300 Å. Extensive low and high angle X-ray diffraction patterns has been performed to structurally characterize the samples. High angle scans clearly showed the Nb(110) and the Pd(111) preferred orientations and allow us to estimate the lattice parameters, $a_{\mathrm{Nb}} = 3.3$ Å for the bcc-Nb and $a_{\mathrm{Pd}} = 3.9$ Å for the fcc-Pd, in agreement with the values reported in literature [20]. Low angle reflectivity measurements on samples deliberately fabricated to perform structural characterization, show a typical interfacial roughness of 12 Å [10].

The superconducting properties, transition temperatures T_c, perpendicular and parallel upper critical magnetic fields $H_{c2\perp}(T)$ and $H_{c2\parallel}(T)$ were resistively measured using a standard dc four-probe technique. The values obtained for the resistivities are independent of the layering and in the range 3–4 $\mu\Omega\,$cm at 10 K. The ratios $\rho_N(T = 300\ \mathrm{K})/\rho_N(T = 10\ \mathrm{K})$, with ρ_N the normal state resistivity, were in the range 1.7–2.2 for all the series confirming the high uniformity of the transport properties in the samples obtained in the same deposition run. Measuring a resistivity value of $\rho_{\mathrm{Nb}} = 2.5\ \mu\Omega\,$cm in the case of a deliberately fabricated 1000 Å thick single Nb film, and assuming a parallel resistor model [21], we deduced $\rho_{\mathrm{Pd}} \approx 5\ \mu\Omega$ cm.

4 Results and discussion

In Figure 1 the critical temperature T_c is reported as a function of d_{Nb} for the $d_{\mathrm{Pd}}/d_{\mathrm{Nb}}/d_{\mathrm{Pd}}$ trilayers. The transition temperature of the sample with $d_{\mathrm{Nb}} = 200$ Å is not reported since it was below 1.75 K, the lowest temperature reachable with our experimental setup. The temperature asymptotic value of 8.8 K for our bulk Nb is reached above 1500 Å while, below 450 Å, T_c is sensitively reduced. Moreover in Figure 1 the transition temperatures $T_c(d_{\mathrm{Nb}})$ are compared to those of single Nb films, clearly indicating that the suppression of the critical temperatures of the trilayers comes indeed from the proximity effect rather than from the T_c thickness dependence of single Nb. Figure 2 shows T_c vs. d_{Pd}^{in} measurements performed on the $d_{\mathrm{Pd}}^{out}/d_{\mathrm{Nb}}/d_{\mathrm{Pd}}^{in}/d_{\mathrm{Nb}}/d_{\mathrm{Pd}}^{out}$ systems. With increasing d_{Pd}^{in} the critical temperature is lowered until a non monotonic behaviour with a minimum for $d_{\mathrm{Pd}}^{in} \approx 140$ Å is reached, then the curve levels off to a value of 7.8 K for large d_{Pd}^{in}. A similar behavior, consisting in a dip before reaching the maximum and then the asymptotic value, was found in S/F systems such as V/Fe, V/$\mathrm{Fe}_x\mathrm{V}_{1-x}$ [1],

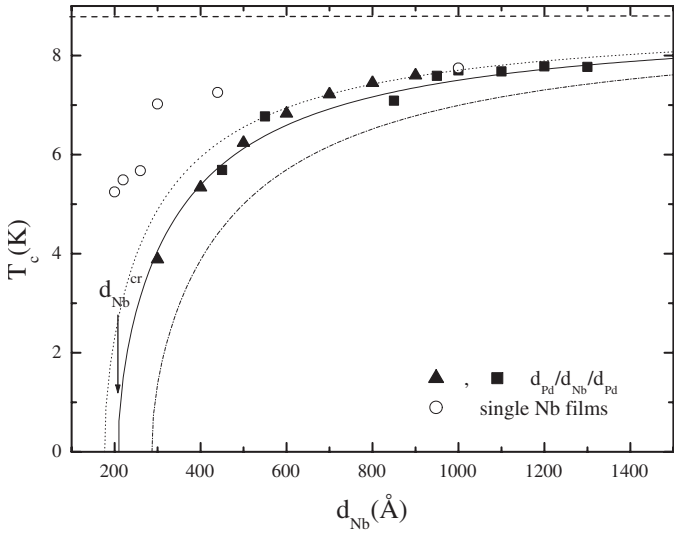

Fig. 1. Critical temperature T_c versus Nb thickness $d_{\rm Nb}$ for $d_{\rm Pd}/d_{\rm Nb}/d_{\rm Pd}$ trilayers (solid symbols). Different symbols refer to sample sets obtained in different deposition runs (set A and set B). Open symbols refer to single Nb films. The dashed line shows the T_c of our bulk Nb. The solid line is the result of the calculations with the parameters given in Table 1. The arrow indicates the value of $d^{cr}_{\rm Nb}$. The dashed and the dot-dashed lines indicate the theoretical calculation for $\mathcal{T} = 0.42$ and $\mathcal{T} = 0.54$, respectively.

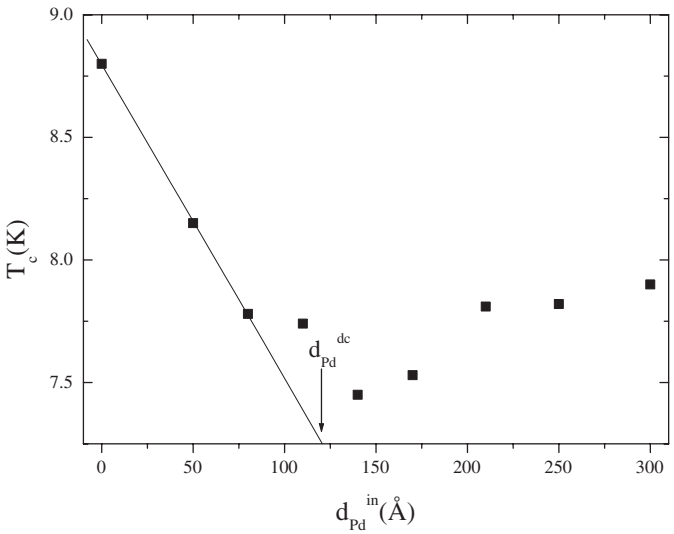

Fig. 2. Critical temperature T_c versus inner Pd thickness $d^{in}_{\rm Pd}$ for sample set C. The arrow shows the value of $d^{dc}_{\rm Pd}$. The line indicates the method used to determinate it.

$\rm Nb/Pd_{1-x}Fe_x/Nb$ [16] and $\rm Nb/Cu_{1-x}Ni_x$ [2,22], and may be related to the strong paramagnetic nature of Pd, such as the abrupt decrease of T_c for small values of $d^{in}_{\rm Pd}$. A qualitatively explanation for the saturation of the $T_c(d^{in}_{\rm Pd})$ curve can be given by considering that when the Nb layers are separated by a thin Pd layer, the decay of Cooper pairs from both sides overlap, the T_c of the system is increased and we say that the Nb layers are coupled. By increasing $d^{in}_{\rm Pd}$ the Nb layers become more and more decoupled and the critical temperature reaches a limiting value related to T_c of the single isolated Nb layer ($d_{\rm Nb} = 500$ Å). We found that this critical temperature value is a little higher than the one obtained for the trilayer with $d_{\rm Nb} = 500$ Å ($T_c \approx 6$ K, see Fig. 1). This is probably due to different deposition conditions, since these two series were fabricated in different deposition runs. Moreover, in the two systems, Nb layers were included in Pd layers of different thickness and this may also play a role. The thickness for which the temperature becomes constant is the decoupling thickness $d^{dc}_{\rm Pd}$. This thickness is related to the coherence length by $d^{dc}_{\rm Pd} \approx 2\,\xi_{\rm Pd}$. We identify $d^{dc}_{\rm Pd}$ extrapolating the steepest slope in the $T_c(d^{in}_{\rm Pd})$ curve to the $d^{in}_{\rm Pd}$ axis (line in Fig. 2) [5]. The value for $\xi_{\rm Pd}$ of approximately 60 Å that we find with this procedure is comparable with other values reported in literature for similar systems [16] while it is considerably lower than the values found for other normal metals, such as Cu [13,22], and greater than values found for the ferromagnetic ones [1,14,15]. In addition this value, in our temperature range, is in agreement with the one estimated from the measured $\rho_{\rm Pd}$ with the expression of $\xi_{\rm Pd}$ valid in the dirty limit:

$$\xi_{\rm Pd} = \sqrt{\frac{\hbar D_{\rm Pd}}{2\pi k_B T}}. \tag{6}$$

Here $D_{\rm Pd}$ is the diffusion coefficient which is related to the low temperature resistivity $\rho_{\rm Pd}$ through the electronic mean free path $l_{\rm Pd}$ by [23]

$$D_{\rm Pd} = \frac{v_{\rm Pd} l_{\rm Pd}}{3} \tag{7}$$

in which

$$l_{\rm Pd} = \frac{1}{v_{\rm Pd}\gamma_{\rm Pd}\rho_{\rm Pd}} \left(\frac{\pi k_B}{e}\right)^2 \tag{8}$$

where $\gamma_{\rm Pd} \approx 11.2 \times 10^2$ J/K^{2}m^3 is the Pd electronic specific heat coefficient [24] and $v_{\rm Pd} = 2.00 \times 10^7$ cm/s is the Pd Fermi velocity [25]. The values obtained for $\xi_{\rm Pd}$ are between 73 Å and 115 Å for $T = 10$ K and $T = 4$ K, respectively, while, from equation (8), $l_{\rm Pd} = 60$ Å. The value of the ratio $l_{\rm Pd}/\xi_{\rm Pd}$, always less than one in the considered temperature range, confirms the validity of the dirty limit approximation.

Inspired by these results we also tried to explain the abrupt decrease and the dip of T_c shown in Figure 2 extending the Radovic theory [26] to the case of S/N systems with N a normal metal with high spin susceptibility. While Radovic's theory well describes this behaviour for both S/F [14,15] and S/M systems [27], we did not obtain a good agreement with the experimental data. However we have to remark that for Nb/Pd multilayers a monotonic decrease of $T_c(d_{\rm Pd})$ was observed [10,16,28]. This behaviour has been discussed in the framework of de Gennes-Werthamer theory, but at the price of supposing very low or, alternatively, very high values of Pd resistivities [10,28].

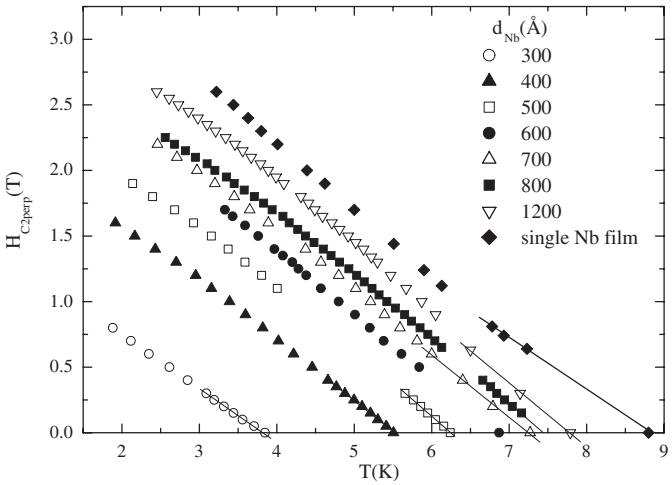

Fig. 3. Perpendicular critical magnetic field for $d_{\rm Pd}/d_{\rm Nb}/d_{\rm Pd}$ trilayers and for a single Nb film. Different symbols represent different $d_{\rm Nb}$, as indicated in the legend. The lines are the result of the linear fits near T_c.

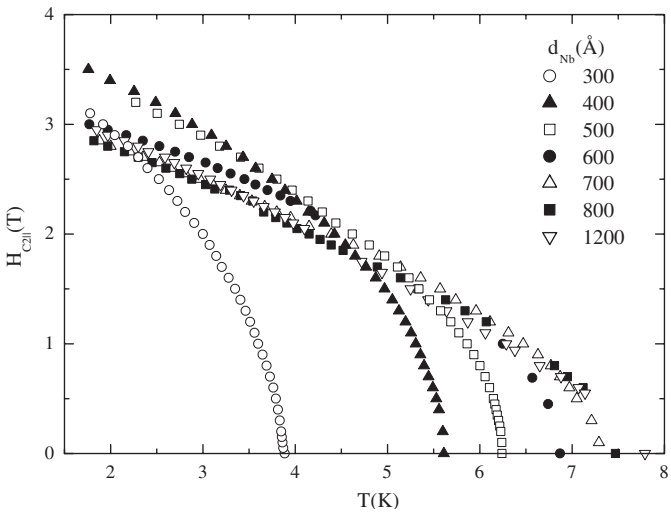

Fig. 4. Parallel critical magnetic field for the same $d_{\rm Pd}/d_{\rm Nb}/d_{\rm Pd}$ trilayers with different $d_{\rm Nb}$, as in Figure 3.

Upper critical fields of $d_{\rm Pd}/d_{\rm Nb}/d_{\rm Pd}$ trilayers were also measured in order to determine $\xi(0)$, the Ginzburg-Landau coherence length at zero temperature, from the slope $S = dH_{C2}/dT|_{T=T_c}$. $\xi_{\rm Nb}$ is, in fact, related to $\xi(0)$ by the relation $\xi_{\rm Nb}$=$2\xi(0)/\pi$. The slope S is extrapolated from the $H_{C2\perp}(T)$ curves by a linear fit near T_c, as shown in Figure 3. A value of about $\xi_{\rm Nb} = 64$ Å was found for single Nb film, 1000 Å thick and this value agrees with the one obtained for samples with thicker Nb interlayers ($d_{\rm Nb} \geq 700$ Å). It is also interesting to note that $H_{C2\perp}(T)$ slopes for the different samples are quite constant, which is a behaviour already observed in S/F systems [14]. In Figure 4 parallel critical magnetic fields are shown. The main feature of these curves is the square root behaviour of $H_{C2\parallel}(T)$ in all the temperature range and the absence of the $3D$−$2D$ crossover. Also this feature may be related to the magnetic nature of Pd. So, from both perpendicular and parallel critical fields measurements seems to emerge that Nb/Pd systems behave more as a S/F rather than a S/N system, even if this indication is not confirmed by T_c's measurements. A similar behaviour was already observed in Nb/Pd multilayers [10]. In this case the critical temperature showed a monotonic decrease as a function of the Pd thickness, which was described in the framework of the classical Gennes-Werthamer proximity theory valid for S/N systems. On the other hand the hypothesis of the Pd ferromagnetic nature seemed to be the reason of the early $3D$−$2D$ dimensional crossover observed in $H_{C2\parallel}(T)$ measurements [10].

With these results for $\xi_{\rm Nb}$ and $\xi_{\rm Pd}$ and with the measured $\rho_{\rm Nb}$ and $\rho_{\rm Pd}$ values reported above it is possible to calculate the proximity effect parameter $\gamma = 0.53$ and to reproduce $T_c(d_{\rm Nb})$ of the trilayers by equation (3) with only one free parameter, γ_b. As reported above in equation (3), the validity regime of the Werthamer approximation is $T_c/T_{cs} \gg \gamma/\gamma_b$. In our case, even if the condition is not fully satisfied, the ratio $\gamma/\gamma_b = 0.4$ is always less than T_c/T_{cs}. In fact T_c/T_{cs}, in the trilayers critical temperatures range, is between 0.5−1. The result of the calculation is shown in Figure 1 (solid line) and it is obtained for $\gamma_b = 1.17$, which means $\mathcal{T} = 0.46$. In Figure 1 are also shown the curves obtained for different $\mathcal{T}$ values ($\mathcal{T} = 0.42$, 0.46, 0.54 from left to right). It is evident that varying $\mathcal{T}$ only of 0.04 the accordance between the theory and the experimental data is completely lost. In addition, motivated by the observed $H_{C2\perp}(T)$ and $H_{C2\parallel}(T)$ behaviours, we tried to reproduce the experimental results with the extended theory for S/F systems [1]. However in this case the best fit to the data is obtained for $\mathcal{T} = 0.86$, which seems to be an unphysical value for the transparency of a real system. Of course if we also identify $\xi_{\rm Pd} \approx d^{dc}_{\rm Pd}$, as recently reported [29,30], the interface transparency will be further increased. In particular we are not able to reproduce the experimental point even if we use $\mathcal{T} = 0.99$. From the curve in Figure 1 it is possible to determine the value of $d^{cr}_{\rm Nb} \approx 200$ Å. In Table 1 are summarized all the samples parameters. The critical thickness normalized to the coherence length in Nb can also be calculated. It depends both on interface transparency and on the strength of the pairing, lowering with increasing $\xi_{\rm Pd}$ and decreasing $\mathcal{T}$. In S/F systems with $\mathcal{T} = 1$, d^{cr}_s/ξ_s has its theoretical upper limit close to 6 [1]. The value we obtained, $d^{cr}_{\rm Nb}/\xi_{\rm Nb} \approx 3$, is comparable to that ($d^{cr}_{\rm Nb}/\xi_{\rm Nb} = 2.69$) reported for $Nb/Cu_{0.915}Mn_{0.085}$ systems having $\mathcal{T} = 0.33$ [13] and sensitively higher than the one found for Nb/Cu ($d^{cr}_{\rm Nb}/\xi_{\rm Nb} = 0.48$) with $\mathcal{T} = 0.29$ [13]. The ratio is lower than ours also for $Nb/Cu_{1-x}Ni_x$, probably due to the little interface transparency of those systems [2,22]. The obtained $\mathcal{T}$ value for Nb/Pd systems is substantially high, although lower than expected on theoretical argument based on Fermi velocities mismatch. The values $v_s \equiv v_{\rm Nb} = 2.73 \times 10^7$ cm/s [31] and $v_n \equiv v_{\rm Pd} = 2.00 \times 10^7$ cm/s [25] in equation (1), in fact, would yield $\mathcal{T} = 0.98$. This happens also for other S/N systems, such as Nb/Cu, where $\mathcal{T}_{\rm exp} \approx 0.29$−$0.33$ [13,22], while $\mathcal{T} = 0.8$ should be expected, for Nb/Al with

Table 1. Values of the electrical resistivities $\rho_{\rm Nb}$ and $\rho_{\rm Pd}$, of the coherence lengths $\xi_{\rm Nb}$ and $\xi_{\rm Pd}$ as experimentally determined and used in the fit procedure to estimate the ratio $d^{cr}_{\rm Nb}/\xi_{\rm Nb}$, and the transparency parameter $\mathcal{T}$.

$\rho_{\rm Nb}$ ($\mu\Omega$ cm)	$\rho_{\rm Pd}$ ($\mu\Omega$ cm)	$\xi_{\rm Nb}$ (Å)	$\xi_{\rm Pd}$ (Å)	$d^{cr}_{\rm Nb}/\xi_{\rm Nb}$	$\mathcal{T}$
2.5	5.0	64	60	3.2	0.46

$\mathcal{T}_{\rm exp} \approx 0.2-0.25$ [13,32] instead of $\mathcal{T} = 0.8$, and for Ta/Al with $\mathcal{T}_{exp} \approx 0.25$ [13]. Another very important factor to have a high $\mathcal{T}$ value is the matching between band-structures of the two metals. This parameter influences transparency even more than Fermi velocities. Conduction electrons in Nb and Pd have both a strong d-character [11,13,25] and this fact would also lead to high values of $\mathcal{T}$. Anyway, as we said, also lattice mismatches play a role. In Nb/Pd systems the growth of the bcc-Nb structure on the fcc-Pd one may induce stress at the interfaces. High values of the interface roughness reported in literature for similar Nb/Pd systems fabricated with different deposition techniques [10,16,28] are consistent with these considerations. In this sense a systematic study of the influence of the fabrication method on interface transparency, as already done on Nb/Cu systems [4], would be interesting. Since preparations methods seem to have a strong influence on $\mathcal{T}$, we could expect to have samples of higher quality, and consequently, of larger transparency using, for example, Molecular Beam Epitaxy (MBE) deposition technique.

5 Conclusions

In conclusion we have studied the proximity effect in Nb/Pd layered systems using the interface transparency as the only free parameter. We obtained a relatively high value for $\mathcal{T}$, higher than the one found for Nb/Cu, in accordance with theoretical considerations about mismatches between Fermi velocities and band-structures of the two metals. Anyway the value obtained for $\mathcal{T}$ can only be indicative: it depends on several factors, such as the way we extracted $\xi_{\rm Pd}$ from the $T_c(d^{in}_{\rm Pd})$ curves neglecting its temperature dependence, the measured values of $\rho_{\rm Nb}$ and $\rho_{\rm Pd}$ and the approximation used to go from γ_b to $\mathcal{T}$. What emerges from this study is that Nb/Pd is, in a sense, an intermediate system between the well known Nb/Cu and other S/F or S/M systems such as Nb/Fe, V/Fe, $\rm Nb/Cu_{1-x}Ni_x$ or Nb/CuMn. The high values of the ratio $d^{cr}_{\rm Nb}/\xi_{\rm Nb}$ and the lack of agreement between Radovic's theory and experimental results can be explained by good interface transparency rather than by magnetic arguments. In this sense it is useful to compare our result with the one obtained for Nb/CuMn. The ratio d^{cr}_s/ξ_s is comparable for the two systems [13]. On the other hand the stronger magnetic nature of CuMn is known and also indirectly demonstrated by Radovic's fit, that well describes the critical temperature behavior for Nb/CuMn multilayers [27] but not for Nb/Pd. This makes us think that Pd-based magnetic alloys are good candidates for studying the S/F proximity problem: very low impurity concentrations will induce ferromagnetic ordering, but should not produce great disorder at the interface. An interesting alloy could be PdNi: the magnetic order starts to appear for a Ni concentration of 2.5%. This makes the alloy stoichiometry easy to control and induces an homogeneous ferromagnetism, with a relatively low Curie temperature [33,34]. In this sense PdNi seems to be more intriguing than CuNi because of the low values of the interface transparency measured in Nb/CuNi systems.

References

1. J. Aarts, J.M.E. Geers, E. Brück, A.A. Golubov, R. Coehoorn, Phys. Rev. B **56**, 2779 (1997)
2. A. Rusanov, R. Boogaard, M. Hesselberth, H. Sellier, J. Aarts, Physica C **369**, 300 (2002).
3. A. Otop, R.W.A. Hendrikx, M.B.S. Hesselberth, C. Chiuhu, A. Lodder, J. Aarts, `cond-mat/0303393`, submitted to Europhys. Lett.
4. C. Attanasio, M.L. Della Rocca, S.L. Prischepa, A. Romano, M. Salvato, submitted to Physica C
5. J.M.E. Geers, M.B.S. Hesselberth, J. Aarts, A.A. Golubov, Phys. Rev. B **64**, 94506 (2001)
6. V.A. Vasko, V.A. Larkin, P.A. Kraus, K.R. Nikolaev, D.E. Grupp, C. A. Nordman, A.M. Goldman, Phys. Rev. Lett. **78**, 1134 (1997)
7. Z.W. Dong, R. Ramesh, T. Venkatesan, M. Johnson, Z.Y. Chen, S.P. Pai, V. Talyansky, R.P. Sharma, R. Shreekala, C.J. Lobb, R.L. Greene, Appl. Phys. Lett. **71**, 1718 (1997)
8. N.C. Yeh, R.P. Vasquez, C.C. Fu, A.V. Samoilov, Y. Li, K. Vakili, Phys. Rev. B **60**, 10522 (1999)
9. Z. Sefrioui, D. Arias, V. Peña, J.E. Villegas, M. Varela, P. Prieto, C. León, J.L. Martinez, J. Santamaria, Phys. Rev. B **67**, 214511 (2003)
10. C. Cirillo, C. Attanasio, L. Maritato, L.V. Mercaldo, S.L. Prischepa, M. Salvato, J. Low Temp. Phys. **130**, 509 (2003)
11. G.J. Nieuwenhuys, Adv. Phys. **24**, 515 (1975)
12. J.E. van Dam, O.K. Andersen, Solid State Commun. **14**, 645 (1974)
13. J.M.E. Geers, Ph.D. thesis, Leiden University, 1999
14. P. Koorevaar, Y. Suzuki, R. Coehoorn, J. Aarts, Phys. Rev. B **49**, 441 (1994)
15. G. Verbanck, C.D. Potter, V. Metlushko, R. Schad, V.V. Moshcalkov, Y. Bruynseraede, Phys. Rev. B **57**, 6029 (1998)
16. M. Schöck, C. Sürgers, H.v. Löhneysen, Eur. Phys. J. B **14**, 1 (2000)
17. M.J.M. de Jong, C.W.J. Beenakker, Phys. Rev. Lett. **74**, 1657 (1995)
18. M.Yu. Kupriyanov, V.F. Lukichev, Sov. Phys. JETP **67**, 1163 (1988)
19. A.A. Golubov, Proc. SPIE **2157**, 353 (1994)
20. C. Kittel, *Introduction to Solid State Physics* (Wiley, New York, 1996)
21. M. Gurvitch, Phys. Rev. B **34**, 540 (1986)
22. G.R. Boogaard, Master Thesis, Leiden University, 2001
23. P.R. Broussard, Phys. Rev. B **43**, 2783 (1991)
24. *Handbook of Chemistry and Physics*, edited by R.C. Weast (The Chemical Rubber Co., Cleveland, 1972)

25. L. Dumoulin, P. Nedellec, P.M. Chaikin, Phys. Rev. Lett. **47**, 208 (1981)
26. Z. Radovic, M. Ledvij, L. Dobrosavljevic-Grujic, A.I. Buzdin, J.R. Clem, Phys. Rev. B **44**, 759 (1991)
27. C. Attanasio, C. Coccorese, L.V. Mercaldo, S.L. Prischepa, M. Salvato, L. Maritato, Phys. Rev. B **57**, 14411 (1998)
28. S. Kaneko, U. Hiller, J.M. Slaughter, C.M. Falco, C. Coccorese, L. Maritato, Phys. Rev. B **58**, 8229 (1998)
29. L.R. Tagirov, Physica C **307**, 145 (1998)
30. Ya.V. Fominov, N.M. Chtchelkatchev, A.A. Golubov, Phys. Rev. B **66**, 14507 (2002)
31. H.R. Kerchner, D.K. Christen, S.T. Sekula, Phys. Rev. B **24**, 1200 (1981)
32. A.A. Golubov, E.P. Houwman, J.G. Gijsbertsen, V.M. Krasnov, J. Flokstra, H. Rogalla, M.Yu. Kupriyanov, Phys. Rev. B **51**, 1073 (1995)
33. T. Kontos, M. Aprili, J. Lesueur, X. Grison, Phys. Rev. Lett. **86**, 304 (2000)
34. T. Kontos, M. Aprili, J. Lesueur, F. Genêt, B. Stephanidis, R. Boursier, Phys. Rev. Lett. **89**, 137007 (2002)